Report

Current Biology

Metabolic tradeoffs control biodiversity gradients through geological time

Highlights

- There is a non-monotonic relationship between climate and biodiversity through time
- Thermodynamics and physiology explain this temperature-biodiversity relationship
- Aerobic scope likely limits low-latitude biodiversity on geologic timescales
- Low-latitude ecosystems are particularly at risk under future climate projections

Authors

Thomas H. Boag, William Gearty, Richard G. Stockey

Correspondence

thomas.boag@yale.edu

In brief

Boag et al. demonstrate a non-monotonic relationship between temperature and diversity over the last 145 million years. By combining principles of thermodynamics and physiology, they derive a model that predicts this relationship. This suggests that low-latitude ecosystems are particularly vulnerable to future biodiversity loss in the near future.

Boag et al., 2021, Current Biology *31*, 1–8
July 12, 2021
https://doi.org/10.1016/j.cub.2021.04.021

CellPress

Please cite this article in press as: Boag et al., Metabolic tradeoffs control biodiversity gradients through geological time, Current Biology (2021), https://doi.org/10.1016/j.cub.2021.04.021

Current Biology

CellPress

Report

Metabolic tradeoffs control biodiversity gradients through geological time

Thomas H. Boag,[1,2,4,6,*] William Gearty,[1,3,4,5] and Richard G. Stockey[1,4]
[1]Department of Geological Sciences, Stanford University, Stanford, CA 94305, USA
[2]Department of Earth and Planetary Sciences, Yale University, New Haven, CT 06511, USA
[3]School of Biological Sciences, University of Nebraska-Lincoln, Lincoln, NE 68588, USA
[4]These authors contributed equally
[5]Twitter: @willgearty
[6]Lead contact
*Correspondence: thomas.boag@yale.edu
https://doi.org/10.1016/j.cub.2021.04.021

SUMMARY

The latitudinal gradient of increasing marine biodiversity from the poles to the tropics is one of the most conspicuous biological patterns in modern oceans.[1–3] Low-latitude regions of the global ocean are often hotspots of animal biodiversity, yet they are set to be most critically affected by anthropogenic climate change.[4] As ocean temperatures rise and deoxygenation proceeds in the coming centuries, the volume of aerobically viable habitat is predicted to decrease in these zones.[5,6] In contrast to the slightly asymmetrical modern latitudinal biodiversity gradient,[7] compilations of fossil occurrences indicate peaks in biodiversity may have existed much further away from the equator in the past, with transitions between climate states hypothesized to explain this trend.[8–13] We combine a new compilation of fossil mollusc occurrences, paleotemperature proxies, and biogeographic data to reveal a non-monotonic relationship between temperature and diversity in the paleontological record over the last 145 million years. We derive a metabolic model that integrates the kinetic effects of temperature on biodiversity[14] with the recently described Metabolic Index that calculates aerobic habitat availability based on the effect of temperature on hypoxia sensitivity.[5,15,16] Although factors such as coastal habitat area and homeothermy are important,[17,18] we find strong congruence between our metabolic model and our fossil and paleotemperature meta-analysis. We therefore suggest that the effects of ocean temperature on the aerobic scope of marine ectotherms is a primary driver of migrating biodiversity peaks through geologic time and will likely play a role in the restructuring of biodiversity under projected future climate scenarios.

RESULTS

Estimating temperature and biodiversity through time

In our analyses of temperature and biodiversity across the last 145 million years, we divided the globe into 24 equal-area latitudinal bins. We then calculated sea surface temperature and diversity for each of these latitudinal bins across ten time intervals that have been chosen based on the availability of temperature proxy data in the published literature with high-enough temporal and geographic resolution and broad-enough latitudinal spread: the Early Cretaceous (Berriasian to Barremian, 145–125 Ma), Campanian (83.6–72.1 Ma), Maastrichtian (72.1–66 Ma), Late Paleocene (59.2–56 Ma), Early Eocene (56–47.8 Ma), Middle Eocene (47.8–37.8 Ma), Early Oligocene (33.9–27.82 Ma), Late Miocene (Serravallian to Messinian, 13.82–5.333 Ma), Late Pliocene (3.333–2.58 Ma), and Modern. Although there is abundant temperature proxy data for earlier time periods, the data are often limited to very narrow latitudinal ranges. To determine the modern temperature gradient, we used objectively analyzed decadally averaged annual mean sea surface temperature data at one-degree grid resolution spanning 1955 to 2012 from the World Ocean Atlas 2013 V2.[19] To estimate temperature for the nine geological time periods, we obtained sea surface temperature estimates and associated paleolatitude estimates from previous compilations based on terrestrial and marine proxies.[20–23] For each time interval, we fit a generalized additive spline model to the data using generalized cross validation. The model was then used to estimate the average sea surface temperature within each latitudinal bin.

For biodiversity estimates, we used genus-level mollusc occurrences. Molluscs are ideal ectotherms for such analyses due to their widespread geographic extent, abundance across marine ecosystems, and high preservation potential in the fossil record. We chose to estimate genus diversity for both the modern and our geologic time periods, as fossil specimens are very often not attributed to species. Although there has been debate as to whether genera should be used as proxies for species in the fossil record,[24] broad-scale geographic diversity patterns are often similar at both taxonomic levels.[2,25] To calculate modern genus diversity, we downloaded mollusc occurrences from marine shelf environments (less than 200 m water depth) from the Global Biodiversity Information Facility (https://www.gbif.org/occurrence/download/0135238-200613084148143; summarized in Figure 1). To calculate genus diversity in the fossil record, we downloaded fossil mollusc occurrence data from the Paleobiology Database

Please cite this article in press as: Boag et al., Metabolic tradeoffs control biodiversity gradients through geological time, Current Biology (2021), https://doi.org/10.1016/j.cub.2021.04.021

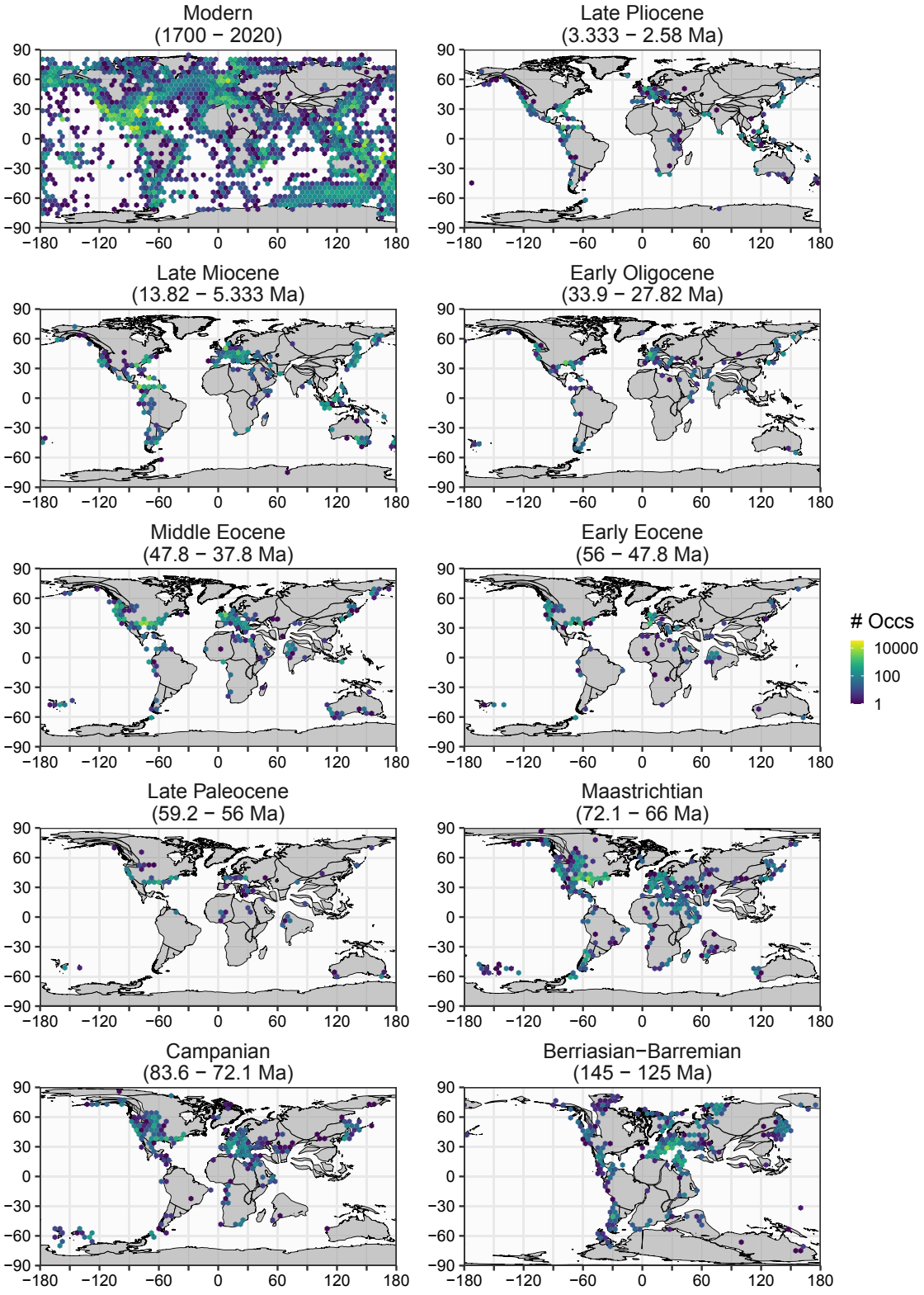

Figure 1. Density of raw mollusc occurrences plotted by time interval

Occurrences are binned within 5-degree by 5-degree hexagons for visualization purposes. Paleogeographic reconstructions are taken from GPlates.[26] See Figures S1A and S1B for a summary of occurrence distributions by latitude and temperature at the meta-analysis level.

Please cite this article in press as: Boag et al., Metabolic tradeoffs control biodiversity gradients through geological time, Current Biology (2021), https://doi.org/10.1016/j.cub.2021.04.021

CellPress

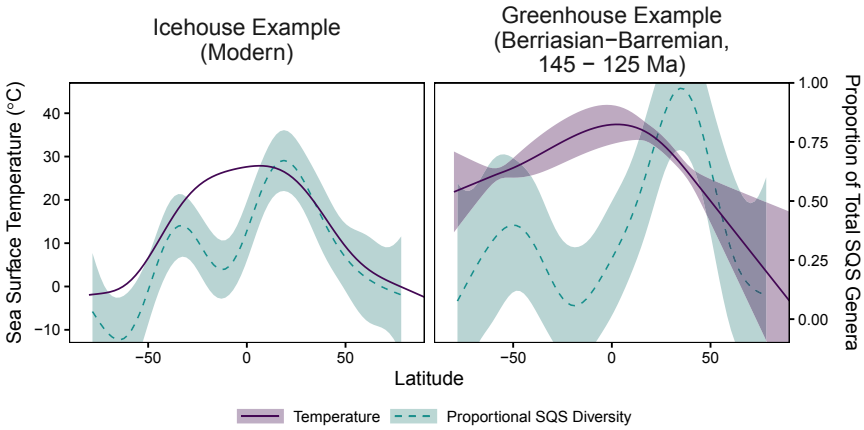

Figure 2. Examples of biodiversity and temperature gradients during cold periods and hot periods

Colored envelopes indicate 95% regression confidence intervals (approximately zero for modern temperature regression). During cold periods (e.g., Modern, maximum average annual temperature is ~28°C, purple solid line), biodiversity (green dashed lines) peaks at low latitudes, but the biodiversity peak migrates to much higher latitudes during hot periods (e.g., Early Cretaceous, maximum average annual temperature is ~37°C). In the greenhouse period, the diversity trough near the equator is further depressed, particularly relative to the diversity peak. See Figure S1C for more details and other time periods. Note that the regressions fit to the diversity data are for illustrative purposes only; we did not interpolate diversity data for any analyses.

(https://paleobiodb.org; summarized in Figure 1). For each time interval, we binned the occurrences within our 24 latitudinal bins using modern latitude or paleolatitude estimates.[26] Despite known geographic sampling biases in the fossil record,[27,28] there is high specimen coverage across all temperatures and latitudes of interest, regardless of binning resolution (Figures S1A and S1B). Then, we used shareholder quorum subsampling (SQS)[29] with a quorum of 0.25 and 100 trials to estimate the generic diversity within each bin. We use this diversity metric to account for uneven preservation and sampling of specimens.[30,31] We show that this specific quorum level (0.25) most effectively accounts for the possible correlation of sampling and diversity, as high diversity can be estimated even with small numbers of specimens (Figure S2A). For each time interval, we also estimated the global generic diversity using SQS with a quorum of 0.25 on the entire occurrence dataset. We divided our latitudinal bin diversity estimates by their respective global diversity estimates to standardize them across time intervals to proportional diversity.

To assess the relationship between temperature and proportional generic diversity since the Cretaceous, we fit nine different regression models to the data: linear; linear with one to four breakpoints; quadratic; cubic; quartic; and a generalized additive spline (GAM). We then compared their fit to the data using the corrected Akaike information criterion (ΔAICc and AICc weights).[32] To address potential concerns regarding SQS or sampling biases, we repeated this model fitting approach using alternative diversity estimation methods and several sampling cutoffs (STAR Methods).

Climate and migration of biodiversity peaks

In total, we had occurrence data for 198 latitude bins across the nine geologic time intervals (Late Pliocene, 20; Late Miocene, 21; Early Oligocene, 17; Middle Eocene, 20; Early Eocene, 15; Late Paleocene, 13; Maastrichtian, 22; Campanian, 22; Berriasian-Barremian, 24) and for the Modern (24 bins). The temperature estimates for these bins range from −2°C to 37°C (271 to 310 K), and the proportional diversity estimates range from 1% to 84%. In time intervals with maximum temperatures below ~27°C (300 K; e.g., Modern, Late Pliocene, and Late Miocene), diversity tends to peak at low latitudes (Figures 2 and S1C; note that the regressions fit to the diversity data are for illustrative purposes only; we did not interpolate diversity data for any analyses). This matches trends observed in many other Modern clades.[2,3] However, time intervals with maximum temperatures greater than ~27°C (300 K) (e.g., Early Eocene, Late Paleocene, and Berriasian-Barremian) tend to exhibit more dramatic decreases in diversity near the equator, with peaks in diversity at higher latitudes (Figures 2 and S1C).[8,10] Although, in general, these latitudinal diversity gradient reconstructions vary between different climate regimes, they also have variation that is likely caused by biases, such as limited sampling. The true diversity patterns may also be impacted by biotic or abiotic factors, such as lack of shallow shelf area, nutrient availability, and biotic interactions. To address these potential sources of variation between time intervals, here, we combine all these latitudinal gradients within our meta-analysis framework to investigate the direct effects of temperature on biodiversity, rather than comparing relative temperature differences reflected by latitude across different climate regimes (Figures 3, S1A, and S1B). Low-diversity estimates occur across the entire temperature range of our meta-analysis but are most pronounced at the extremes. However, high-diversity estimates (>50%) almost exclusively occur in the middle of the temperature range, a trend that is robust to sampling intensity (STAR Methods). Combined, this results in a diversity-temperature relationship that peaks at moderate temperatures (15°C–25°C) and decreases outside of this range.

Our model fitting approach resulted in essentially no support for a simple linear regression to summarize the relationship between proportional diversity and temperature (Table S1), regardless of diversity metric or sampling cutoff (Figure S2B). For the main analysis described above, the model with the best relative fit is a linear regression with a single breakpoint at 18.3°C (291.4 K; ±3.2), with a slope of 0.12 for temperatures below this breakpoint and a slope of −0.03 for temperatures above it (Figure 3). The breakpoint temperature is robust to sampling, diversity metric, and binning method (STAR Methods; Figure S3A). Furthermore, the regression slope for lower temperatures is similarly robust and indistinguishable from the empirical estimate of Roy et al.[1] based on marine prosobranch gastropods and the theoretical range proposed by Gillooly and Allen[33] using the metabolic theory of ecology (STAR Methods; Figure S3B). Other models with substantial support (<2 ΔAICc) include linear regressions with two or three breakpoints and a generalized additive spline. These four models together account for more than 85% of the AICc weight (Table S1).

Please cite this article in press as: Boag et al., Metabolic tradeoffs control biodiversity gradients through geological time, Current Biology (2021), https://doi.org/10.1016/j.cub.2021.04.021

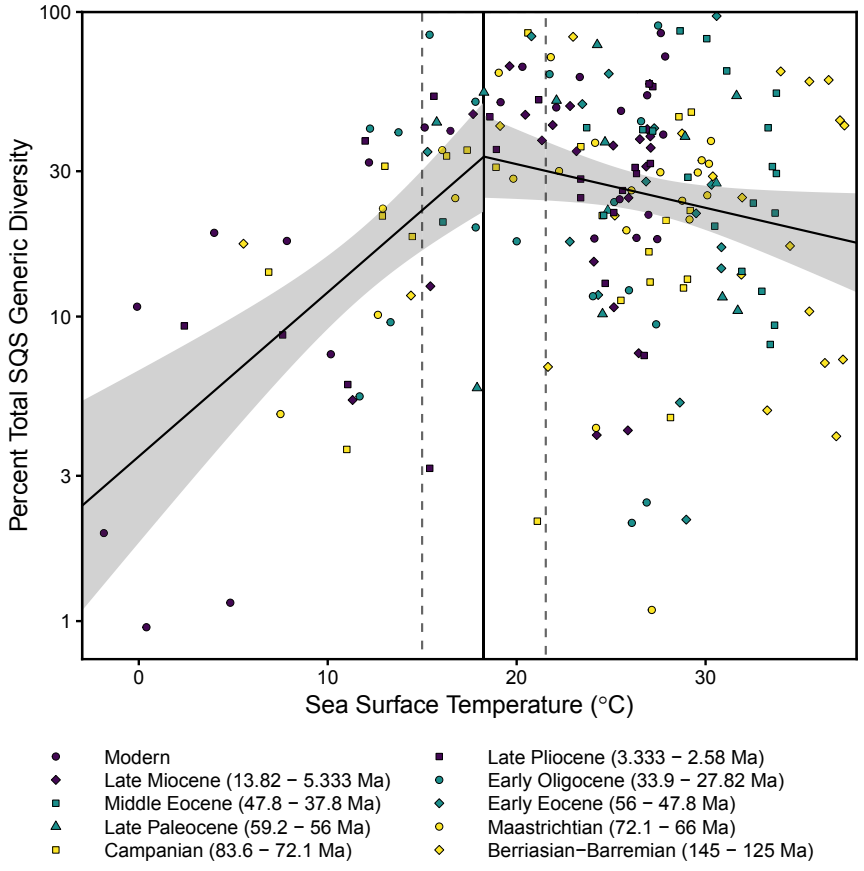

Figure 3. Estimated percent generic diversity and reconstructed temperature across the modern and nine geologic time intervals

Each point represents percent generic diversity in an equal-area latitudinal band from a given time interval, with sea surface temperature for each band determined from proxy data. The independent variable of temperature is therefore explicitly illustrated as a predictor of species diversity across all geological intervals at once. The solid vertical line indicates the best-fitting linear regression breakpoint, with the dotted vertical lines representing ±1.96σ. The black curve represents the best-fitting breakpoint regression, with the gray region representing the 95% confidence interval. See Figures S2 and S3 for sensitivity analysis results.

Temperature-driven metabolic tradeoffs

We developed a novel metabolic model that combines the kinetic relationship between temperature and biodiversity[14,33] and the predicted impact of temperature-dependent hypoxia on aerobic niche availability.[5,15] Specifically, we propose that the change in total taxonomic richness (S_{tot}; Equation 1) per unit temperature (T) is the sum of changes in richness predicted by the temperature dependence of biochemical kinetics (S_{kinet}) and the temperature dependence of aerobic habitat viability (S_{aerob}):

$$\frac{d\ \ln(S_{tot})}{d\ T} = \frac{d\ \ln(S_{kinet})}{d\ T} + \frac{d\ \ln(S_{aerob})}{d\ T} \qquad \text{(Equation 1)}$$

Our expression for S_{kinet} is borrowed directly from Allen et al.[14] (Equation 2), where E is the activation energy of metabolism, k_B is the Boltzmann constant, and C_1 is a temperature-independent constant:

$$\ln(S_{kinet}) = \left(\frac{-E}{1000\ k_B}\right)\left(\frac{1000}{T}\right) + C_1 \qquad \text{(Equation 2)}$$

S_{aerob} is defined based on the Metabolic Index, a method developed to quantify the extent of viable aerobic habitat for marine ectotherms (Equation 3):

$$S_{aerob} = \sum A_o \frac{pO_2}{\exp\left[\frac{-E_o}{k_B}\left(\frac{1}{T} - \frac{1}{T_{ref}}\right)\right]} > \phi_{crit} \qquad \text{(Equation 3)}$$

A_o and E_o are species-specific physiological traits. A_o is the inverse of a species' hypoxic threshold (i.e., the minimum pO_2 at which resting metabolism can be sustained), and E_o is the temperature dependency of A_o. ϕ_{crit} is the ratio of the energy required to sustain key ecological activities versus resting metabolism. ϕ_{crit} is estimated based on the biogeographic distribution of taxa for which A_o and E_o are known. T_{ref} is a reference temperature of 15°C, and pO_2 is the partial pressure of oxygen in seawater.

We use a Monte Carlo approach to generate uncertainty-bounded predictions of diversity-temperature relationships in marine ectotherms. E (Equation 2), the slope of the linear relationship defining $\frac{d\ \ln(S_{Kinet})}{d\ (1000/T)}$ in Allen et al.,[14] is parameterized by a uniform distribution describing updated calculations and associated uncertainty for the activation energy of metabolism.[33] A_o, E_o, and ϕ_{crit} are all individually parameterized using probability density functions that describe the physiological responses of 61 different marine ectotherm species (described in Penn et al.[15] and Table S2). pO_2 is parameterized by a uniform distribution defined by the 5th and 95th percentiles of observed modern sea surface values.[34] Initial $\ln(S_{tot})$ values are defined based on our best fit model and associated uncertainty presented in Figure 3, calibrating the relative predicted changes in biodiversity with temperature from our model to observed data. We specifically highlight how the temperature sensitivity of hypoxic thresholds (E_o; Equation 3) relates to predicted biodiversity-temperature relationships. We therefore solve our model at E_o values corresponding to the mean, mean ± 0.5σ, and mean ± 1σ of the normal distribution (Table S2) to produce the analyses presented in Figure 4. See STAR Methods for further details of Monte Carlo approach and methods for solving differential equations. We additionally present distributions of modeled annual mean equatorial sea surface temperature (summarizing spatial variation) from the HadGEM2-ES Earth system model[35] for preindustrial climate (based upon the year 1860) and Representative/Extended Concentration Pathways 4.5 and 8.5[36,37] for the years 2100 and 2299, to aid comparison between our results and future projected sea surface temperatures (Figure 4).

Please cite this article in press as: Boag et al., Metabolic tradeoffs control biodiversity gradients through geological time, Current Biology (2021), https://doi.org/10.1016/j.cub.2021.04.021

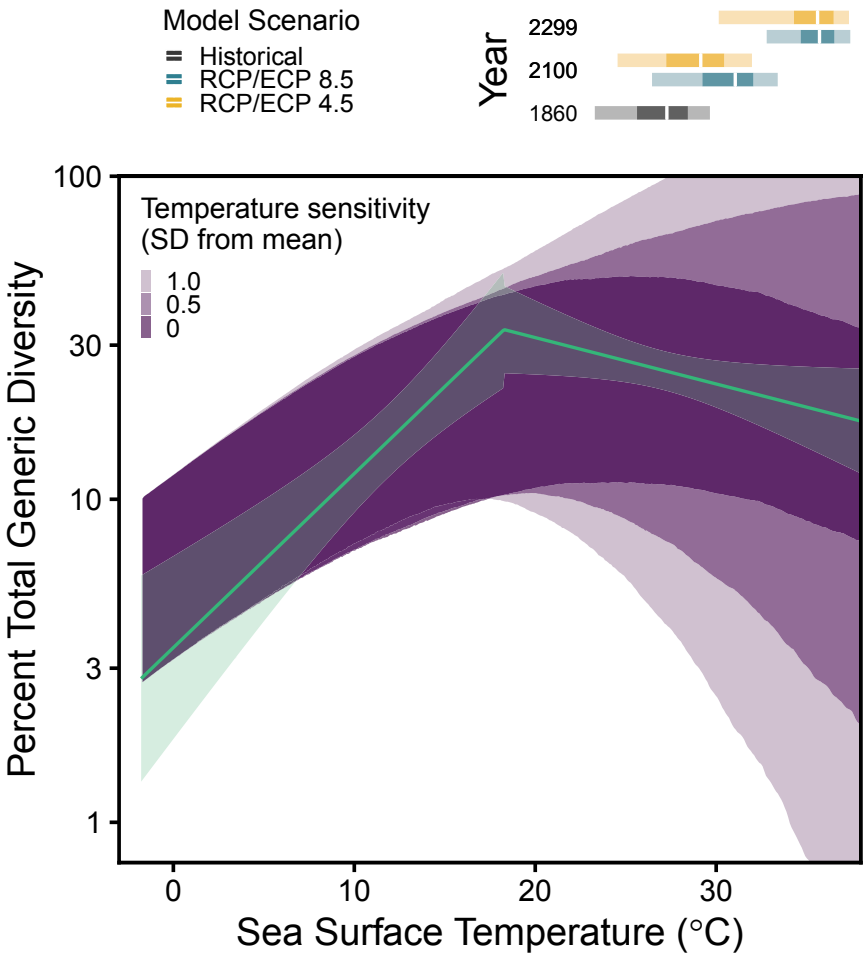

Figure 4. Combined metabolic model describing predicted relationships between biodiversity and temperature

The dark purple envelope describes 2 SD estimates of diversity for mean E_o (temperature sensitivity of hypoxic threshold). Lighter purple envelopes illustrate the increased uncertainty of predicted diversity with 0.5 and 1 SD from mean temperature sensitivity. Green line shows the observed relationship between percent generic diversity and temperature as summarized in Figure 3. Above the model, we illustrate the distributions of monthly equatorial sea-surface temperatures predicted for the years 2100 and 2299 under Representative and Extended Concentration Pathways (RCP/ECP) 4.5 and 8.5, relative to historical model temperatures for 1860 from the HadGEM2-ES model. Vertical white lines represent median values across the global surface ocean, darker bars represent interquartile ranges of spatial temperature variation, and lighter bars represent 5th and 95th percentiles. See Figure S4 for results of sensitivity analysis using temperature sensitivity of individual mollusc species.

Our combined metabolic model predicts the first-order relationship between temperature and marine biodiversity that we observe in our analyses of primary data (Figure 4). The model supports an approximately exponential increase in proportional biodiversity below 20°C–25°C, in agreement with the metabolic theory of ecology.[14] At higher temperatures, aerobic limitation becomes a dominant control and predicted biodiversity begins to decline with increasing temperature, matching well with our observations from the fossil record (Figure 4). At extreme temperature sensitivities, our model can accommodate both a continuous monotonic increase in diversity, as predicted by the metabolic theory of ecology,[14] and a precipitous drop, as predicted by the Metabolic Index,[5,15,16] but both of these scenarios are unlikely, given the modern distributions of temperature sensitivities.[15,16] Of the 61 marine ectotherms used to construct the probability density functions defining the E_o, A_o, and ϕ_{crit} distributions used in the Monte Carlo model, 7 are molluscs. However, we propose (as previous authors have)[15] that the improved sampling density of modern physiological responses that we gain from including non-molluscan taxa improves the accuracy of our model relative to using molluscan data alone. We further demonstrate that we can capture the full range of temperature-diversity relationships shown in Figure 3 using the individual mollusc E_o values from the Penn et al.[15] dataset (Figure S4).

DISCUSSION

Although this study evaluates marine biodiversity from the late Mesozoic through Cenozoic, the principles laid out here may also serve as a framework for interpreting the role of climate change and physiology in driving biodiversity trends deeper into the Phanerozoic. For example, combined Earth system and ecophysiological modeling of the Permian-Triassic extinction suggests temperature-dependent hypoxia tolerance predicts the latitudinal loss of biodiversity observed across the boundary.[15] Furthermore, the flattened overall biodiversity gradient in the early Triassic[38] can be linked to persistently higher sea surface temperatures (>30°C–40°C) than those in the modern equatorial ocean,[39–41] as well as the potentially compounding effects of widespread ocean deoxygenation.[15,42] Expanding studies like these to wider intervals of the geologic record has exciting potential but in many cases would require the generation of considerably more geochemical data (and potentially more paleontological data).

In deep time, peaks in latitudinal biodiversity broadly correspond with climate state;[10] however, these patterns may also be impacted by other factors, such as continental shelf area[43] and continental configuration.[44,45] Also, there are inherent biases associated with reconstructing these patterns of biodiversity from the fossil record, including anthropogenic search intensity and geographic sampling,[46] taxonomic classification,[47] animals with hard parts preserving better than soft-bodied groups,[48] and time averaging of assemblages as they enter the fossil record.[49] Furthermore, when reconstructing paleotemperatures, marine and terrestrial environments may record slightly different temperature histories, proxy data are unlikely to have sufficient resolution to examine the impact of seasonality, and individual

Please cite this article in press as: Boag et al., Metabolic tradeoffs control biodiversity gradients through geological time, Current Biology (2021), https://doi.org/10.1016/j.cub.2021.04.021

paleotemperature proxies have system-specific uncertainties (e.g., the $\delta^{18}O$ proxy may be impacted by assumptions regarding seawater isotope values and diagenetic alteration).[50,51] Despite these possible sources of uncertainty, our use of comprehensive paleontological data and spatially extensive paleotemperature proxy data within a meta-analysis framework has revealed a strong connection between temperature and diversity through Earth history.

Looking toward future climate projections, increases in greenhouse gas concentrations leading to a global mean warming of ~0.75°C to 2.75°C by the end of the 21st century (Representative Concentration Pathways 2.6–8.5; Figure 4)[36] will likely result in continued dissolved oxygen loss and up to 6°C warming of the upper tropical ocean by 2300 (Extended Concentration Pathway 8.5; Figure 4).[37] These changes will place many tropical species with already limited acclimation potential[52] at temperature and oxygen conditions that are beyond their aerobic thresholds.[53] At an ecosystem scale, this loss of aerobic scope will likely affect biodiversity through disruption of complete life cycles, including predator-prey dynamics, ontogeny, and reproduction, in addition to fragmentation of suitable physiological habitats via poleward migration to extratropical latitudes (>35°).[5,54–56] Other factors, such as declines in primary production, ocean acidification, overfishing, and dead zone expansion, are also expected to exacerbate the effects of warming and deoxygenation.[57–60] Given the expected impacts of these stressors, it remains a critical unanswered question whether the loss of tropical marine biodiversity will be recovered in the coming centuries by long-term acclimation and physiological adaptation.[60,61]

Our paleotemperature data compilation reveals that models of upper ocean temperatures for 2300 predict similar thermal maxima as those measured during hyperthermal events in the geological record, such as the Paleocene-Eocene Thermal Maximum and Early and Latest Cretaceous (Figures 4 and S1C). Furthermore, fossil latitudinal biodiversity gradients of molluscs from the past 145 million years show that, over geological timescales, warmer-than-modern ocean climates with sea surface temperatures above 24°C–27°C result in the permanent extirpation of species richness from tropical latitudes proportional to absolute seawater temperature. Our model results demonstrate that temperature-driven loss of aerobic scope explains this pattern (Figure 4). Of course, many other factors are also expected to negatively impact habitat viability during hyperthermal events, such as physical changes to coral reef habitats (e.g., the impacts of reef accumulation rates and structural complexity on total habitat area and volume);[62,63] however, our results demonstrate that metabolism alone can account for a significant portion of the observed trends. Given the geological timescale of these patterns (millions of years), this suggests that physiological adaptation of marine ectothermic animals is insufficient to allow the repopulation of tropical latitudes during hyperthermal intervals.[56] These findings suggest that contemporary emissions-driven warming will likely result in a comparable loss of biodiversity in the tropical ocean as ecosystems increasingly suffer from the chronic impacts of warming in the coming centuries, a trend that may have already begun.[12]

STAR★METHODS

Detailed methods are provided in the online version of this paper and include the following:

- KEY RESOURCES TABLE
- RESOURCE AVAILABILITY
  - Lead contact
  - Materials availability
  - Data and code availability
- EXPERIMENTAL MODEL AND SUBJECT DETAILS
- METHOD DETAILS
  - Sampling Coverage
  - Diversity Sensitivity Analyses
- QUANTIFICATION AND STATISTICAL ANALYSIS
  - Diversity Sensitivity Analyses

SUPPLEMENTAL INFORMATION

Supplemental information can be found online at https://doi.org/10.1016/j.cub.2021.04.021.

ACKNOWLEDGMENTS

We thank Jonathan Payne, Erik Sperling, and Kate Lyons for helpful discussion contributing to this manuscript. We also thank Moriaki Yasuhara and two anonymous reviewers for insightful feedback during review. T.H.B. thanks support from a NSERC Doctoral Fellowship. R.G.S. acknowledges National Science Foundation grant EAR-1922966 for support. Some of the computing for this project was performed on the Sherlock cluster. We would like to thank Stanford University and the Stanford Research Computing Center for providing computational resources and support that contributed to these research results. We are indebted to the contributors of the Paleobiology Database. This is Paleobiology Database publication 396.

AUTHOR CONTRIBUTIONS

T.H.B. conceived of the project, and all authors designed the research approach. W.G. performed the diversity and temperature analyses with input from T.H.B. and R.G.S. R.G.S. performed the metabolic modeling analyses with input from T.H.B. and W.G. All authors wrote and edited the manuscript.

DECLARATION OF INTERESTS

The authors declare no competing interests.

Received: October 13, 2020
Revised: February 24, 2021
Accepted: April 9, 2021
Published: May 6, 2021

REFERENCES

1. Roy, K., Jablonski, D., Valentine, J.W., and Rosenberg, G. (1998). Marine latitudinal diversity gradients: tests of causal hypotheses. Proc. Natl. Acad. Sci. USA *95*, 3699–3702.
2. Hillebrand, H. (2004). On the generality of the latitudinal diversity gradient. Am. Nat. *163*, 192–211.
3. Willig, M.R., Kaufman, D.M., and Stevens, R.D. (2003). Latitudinal gradients of biodiversity: pattern, process, scale, and synthesis. Annu. Rev. Ecol. Evol. Syst. *34*, 273–309.
4. Ramírez, F., Afán, I., Davis, L.S., and Chiaradia, A. (2017). Climate impacts on global hot spots of marine biodiversity. Sci. Adv. *3*, e1601198.

5. Deutsch, C., Ferrel, A., Seibel, B., Pörtner, H.O., and Huey, R.B. (2015). Ecophysiology. Climate change tightens a metabolic constraint on marine habitats. Science *348*, 1132–1135.
6. Breitburg, D., Levin, L.A., Oschlies, A., Grégoire, M., Chavez, F.P., Conley, D.J., Garçon, V., Gilbert, D., Gutiérrez, D., Isensee, K., et al. (2018). Declining oxygen in the global ocean and coastal waters. Science *359*, eaam7240.
7. Powell, M.G., Beresford, V.P., and Colaianne, B.A. (2012). The latitudinal position of peak marine diversity in living and fossil biotas. J. Biogeogr. *39*, 1687–1694.
8. Reddin, C.J., Kocsis, Á.T., and Kiessling, W. (2018). Marine invertebrate migrations trace climate change over 450 million years. Glob. Ecol. Biogeogr. *27*, 704–713.
9. Kröger, B. (2018). Changes in the latitudinal diversity gradient during the Great Ordovician Biodiversification Event. Geology *46*, 127–130.
10. Mannion, P.D., Upchurch, P., Benson, R.B.J., and Goswami, A. (2014). The latitudinal biodiversity gradient through deep time. Trends Ecol. Evol. *29*, 42–50.
11. Chaudhary, C., Saeedi, H., and Costello, M.J. (2016). Bimodality of latitudinal gradients in marine species richness. Trends Ecol. Evol. *31*, 670–676.
12. Yasuhara, M., Wei, C.-L., Kucera, M., Costello, M.J., Tittensor, D.P., Kiessling, W., Bonebrake, T.C., Tabor, C.R., Feng, R., Baselga, A., et al. (2020). Past and future decline of tropical pelagic biodiversity. Proc. Natl. Acad. Sci. USA *117*, 12891–12896.
13. Yasuhara, M., Hunt, G., Cronin, T.M., and Okahashi, H. (2009). Temporal latitudinal-gradient dynamics and tropical instability of deep-sea species diversity. Proc. Natl. Acad. Sci. USA *106*, 21717–21720.
14. Allen, A.P., Brown, J.H., and Gillooly, J.F. (2002). Global biodiversity, biochemical kinetics, and the energetic-equivalence rule. Science *297*, 1545–1548.
15. Penn, J.L., Deutsch, C., Payne, J.L., and Sperling, E.A. (2018). Temperature-dependent hypoxia explains biogeography and severity of end-Permian marine mass extinction. Science *362*, eaat1327.
16. Deutsch, C., Penn, J.L., and Seibel, B. (2020). Metabolic trait diversity shapes marine biogeography. Nature *585*, 557–562.
17. Tittensor, D.P., Mora, C., Jetz, W., Lotze, H.K., Ricard, D., Berghe, E.V., and Worm, B. (2010). Global patterns and predictors of marine biodiversity across taxa. Nature *466*, 1098–1101.
18. Grady, J.M., Maitner, B.S., Winter, A.S., Kaschner, K., Tittensor, D.P., Record, S., Smith, F.A., Wilson, A.M., Dell, A.I., Zarnetske, P.L., et al. (2019). Metabolic asymmetry and the global diversity of marine predators. Science *363*, eaat4220.
19. Locarnini, R.A., Mishonov, A.V., Antonov, J.I., Boyer, T.P., Garcia, H.E., Baranova, O.K., Zweng, M.M., Paver, C.R., Reagan, J.R., Johnson, D.R., et al. (2013). World Ocean Atlas 2013. Volume 1, Temperature, S. Levitus and A. Mishonov, eds. (NOAA).
20. Herbert, T.D., Lawrence, K.T., Tzanova, A., Peterson, L.C., Caballero-Gill, R., and Kelly, C.S. (2016). Late Miocene global cooling and the rise of modern ecosystems. Nat. Geosci. *9*, 843–847.
21. Littler, K., Robinson, S.A., Bown, P.R., Nederbragt, A.J., and Pancost, R.D. (2011). High sea-surface temperatures during the Early Cretaceous Epoch. Nat. Geosci. *4*, 169–172.
22. van Hinsbergen, D.J.J., de Groot, L.V., van Schaik, S.J., Spakman, W., Bijl, P.K., Sluijs, A., Langereis, C.G., and Brinkhuis, H. (2015). A paleolatitude calculator for paleoclimate studies. PLoS ONE *10*, e0126946.
23. Zhang, L., Hay, W.W., Wang, C., and Gu, X. (2019). The evolution of latitudinal temperature gradients from the latest Cretaceous through the present. Earth Sci. Rev. *189*, 147–158.
24. Hendricks, J.R., Saupe, E.E., Myers, C.E., Hermsen, E.J., and Allmon, W.D. (2014). The generification of the fossil record. Paleobiology *40*, 511–528.
25. Foote, M., Ritterbush, K.A., and Miller, A.I. (2016). Geographic ranges of genera and their constituent species: Structure, evolutionary dynamics, and extinction resistance. Paleobiology *42*, 269–288.
26. Wright, N., Zahirovic, S., Müller, R.D., and Seton, M. (2013). Towards community-driven paleogeographic reconstructions: integrating open-access paleogeographic and paleobiology data with plate tectonics. Biogeosciences *10*, 1529–1541.
27. Vilhena, D.A., and Smith, A.B. (2013). Spatial bias in the marine fossil record. PLoS ONE *8*, e74470.
28. Close, R.A., Benson, R.B.J., Saupe, E.E., Clapham, M.E., and Butler, R.J. (2020). The spatial structure of Phanerozoic marine animal diversity. Science *368*, 420–424.
29. Alroy, J. (2010). The shifting balance of diversity among major marine animal groups. Science *329*, 1191–1194.
30. Close, R.A., Evers, S.W., Alroy, J., and Butler, R.J. (2018). How should we estimate diversity in the fossil record? Testing richness estimators using sampling-standardised discovery curves. Methods Ecol. Evol. *9*, 1386–1400.
31. Bush, A.M., Markey, M.J., and Marshall, C.R. (2004). Removing bias from diversity curves: the effects of spatially organized biodiversity on sampling-standardization. Paleobiology *30*, 666–686.
32. Burnham, K.P., and Anderson, D.R. (2002). Model Selection and Multimodel Inference (Springer).
33. Gillooly, J.F., and Allen, A.P. (2007). Linking global patterns in biodiversity to evolutionary dynamics using metabolic theory. Ecology *88*, 1890–1894.
34. Boag, T.H., Stockey, R.G., Elder, L.E., Hull, P.M., and Sperling, E.A. (2018). Oxygen, temperature and the deep-marine stenothermal cradle of Ediacaran evolution. Proc. Biol. Sci. *285*, 20181724.
35. Jones, C.D., Hughes, J.K., Bellouin, N., Hardiman, S.C., Jones, G.S., Knight, J., Liddicoat, S., O'Connor, F.M., Andres, R.J., Bell, C., et al. (2011). The HadGEM2-ES implementation of CMIP5 centennial simulations. Geosci. Model Dev. *4*, 543–570.
36. Moss, R.H., Edmonds, J.A., Hibbard, K.A., Manning, M.R., Rose, S.K., van Vuuren, D.P., Carter, T.R., Emori, S., Kainuma, M., Kram, T., et al. (2010). The next generation of scenarios for climate change research and assessment. Nature *463*, 747–756.
37. Meinshausen, M., Smith, S.J., Calvin, K., Daniel, J.S., Kainuma, M.L.T., Lamarque, J.-F., Matsumoto, K., Montzka, S.A., Raper, S.C.B., Riahi, K., et al. (2011). The RCP greenhouse gas concentrations and their extensions from 1765 to 2300. Clim. Change *109*, 213–241.
38. Song, H., Huang, S., Jia, E., Dai, X., Wignall, P.B., and Dunhill, A.M. (2020). Flat latitudinal diversity gradient caused by the Permian-Triassic mass extinction. Proc. Natl. Acad. Sci. USA *117*, 17578–17583.
39. Sun, Y., Joachimski, M.M., Wignall, P.B., Yan, C., Chen, Y., Jiang, H., Wang, L., and Lai, X. (2012). Lethally hot temperatures during the Early Triassic greenhouse. Science *338*, 366–370.
40. Romano, C., Goudemand, N., Vennemann, T.W., Ware, D., Schneebeli-Hermann, E., Hochuli, P.A., Brühwiler, T., Brinkmann, W., and Bucher, H. (2013). Climatic and biotic upheavals following the end-Permian mass extinction. Nat. Geosci. *6*, 57–60.
41. Trotter, J.A., Williams, I.S., Nicora, A., Mazza, M., and Rigo, M. (2015). Long-term cycles of Triassic climate change: a new $\delta^{18}O$ record from conodont apatite. Earth Planet. Sci. Lett. *415*, 165–174.
42. Lau, K.V., Maher, K., Altiner, D., Kelley, B.M., Kump, L.R., Lehrmann, D.J., Silva-Tamayo, J.C., Weaver, K.L., Yu, M., and Payne, J.L. (2016). Marine anoxia and delayed Earth system recovery after the end-Permian extinction. Proc. Natl. Acad. Sci. USA *113*, 2360–2365.
43. Reddin, C.J., Kocsis, Á.T., and Kiessling, W. (2019). Climate change and the latitudinal selectivity of ancient marine extinctions. Paleobiology *45*, 70–84.
44. Naimark, E.B., and Markov, A.V. (2011). Northward shift in faunal diversity: a general pattern of evolution of the Phanerozoic marine biota. Biol. Bull. Rev. *1*, 71–81.
45. Saupe, E.E., Qiao, H., Donnadieu, Y., Farnsworth, A., Kennedy-Asser, A.T., Ladant, J.-B., Lunt, D.J., Pohl, A., Valdes, P., and Finnegan, S. (2020). Extinction intensity during Ordovician and Cenozoic glaciations explained by cooling and palaeogeography. Nat. Geosci. *13*, 65–70.

46. Smith, A.B., and McGowan, A.J. (2007). The shape of the phanerozoic marine palaeodiversity curve: How much can be predicted from the sedimentary rock record of Western Europe? Palaeontology *50*, 765–774.

47. Lloyd, G.T., Young, J.R., and Smith, A.B. (2012). Taxonomic structure of the fossil record is shaped by sampling bias. Syst. Biol. *61*, 80–89.

48. Allison, P., and Bottjer, D. (2010). Taphonomy: Process and Bias through Time (Springer).

49. Kowalewski, M. (1996). Time-averaging, overcompleteness, and the geological record. J. Geol. *104*, 317–326.

50. Mills, B.J.W., Krause, A.J., Scotese, C.R., Hill, D.J., Shields, G.A., and Lenton, T.M. (2019). Modelling the long-term carbon cycle, atmospheric CO_2, and Earth surface temperature from late Neoproterozoic to present day. Gondwana Res. *67*, 172–186.

51. Ryb, U., and Eiler, J.M. (2018). Oxygen isotope composition of the Phanerozoic ocean and a possible solution to the dolomite problem. Proc. Natl. Acad. Sci. USA *115*, 6602–6607.

52. Stillman, J.H. (2003). Acclimation capacity underlies susceptibility to climate change. Science *301*, 65.

53. Pörtner, H.O., and Knust, R. (2007). Climate change affects marine fishes through the oxygen limitation of thermal tolerance. Science *315*, 95–97.

54. Sperling, E.A., Frieder, C.A., and Levin, L.A. (2016). Biodiversity response to natural gradients of multiple stressors on continental margins. Proc. Biol. Sci. *283*, 20160637.

55. Danovaro, R., Gambi, C., Dell'Anno, A., Corinaldesi, C., Fraschetti, S., Vanreusel, A., Vincx, M., and Gooday, A.J. (2008). Exponential decline of deep-sea ecosystem functioning linked to benthic biodiversity loss. Curr. Biol. *18*, 1–8.

56. Saupe, E.E., Hendricks, J.R., Portell, R.W., Dowsett, H.J., Haywood, A., Hunter, S.J., and Lieberman, B.S. (2014). Macroevolutionary consequences of profound climate change on niche evolution in marine molluscs over the past three million years. Proc. Biol. Sci. *281*, 20141995.

57. Moore, J.K., Fu, W., Primeau, F., Britten, G.L., Lindsay, K., Long, M., Doney, S.C., Mahowald, N., Hoffman, F., and Randerson, J.T. (2018). Sustained climate warming drives declining marine biological productivity. Science *359*, 1139–1143.

58. Payne, J.L., Bush, A.M., Heim, N.A., Knope, M.L., and McCauley, D.J. (2016). Ecological selectivity of the emerging mass extinction in the oceans. Science *353*, 1284–1286.

59. Diaz, R.J., and Rosenberg, R. (2008). Spreading dead zones and consequences for marine ecosystems. Science *321*, 926–929.

60. Branch, T.A., DeJoseph, B.M., Ray, L.J., and Wagner, C.A. (2013). Impacts of ocean acidification on marine seafood. Trends Ecol. Evol. *28*, 178–186.

61. Sunday, J.M., Crim, R.N., Harley, C.D.G., and Hart, M.W. (2011). Quantifying rates of evolutionary adaptation in response to ocean acidification. PLoS ONE *6*, e22881.

62. Glynn, P.W., and D'Croz, L. (1990). Experimental evidence for high temperature stress as the cause of El Niño-coincident coral mortality. Coral Reefs *8*, 181–191.

63. Knudby, A., LeDrew, E., and Newman, C. (2007). Progress in the use of remote sensing for coral reef biodiversity studies. Prog. Phys. Geogr. *31*, 421–434.

64. R Development Core Team (2019). R: A language and environment for statistical computing (R Foundation for Statistical Computing).

65. Chamberlain, S., Barve, V., Mcglinn, D., Oldoni, D., Desmet, P., Geffert, L., and Ram, K. (2020). rgbif: interface to the global biodiversity information facility API. R Packag. version 3.4.0. https://cran.r-project.org/web/packages/rgbif/index.html.

66. Wickham, H. (2011). The split-apply-combine strategy for data analysis. J. Stat. Softw. *40*, 1–29.

67. Wickham, H., François, R., Henry, L., Müller, K., and Studio, R. (2020). dplyr: a grammar of data manipulation. R Packag. version 1.0.2. https://cran.r-project.org/web/packages/dplyr/index.html.

68. Hijmans, R.J., van Etten, J., Sumner, M., Cheng, J., Baston, D., Bevan, A., Bivand, R., Busetto, L., Canty, M., Fasoli, B., et al. (2020). raster: geographic data analysis and modeling. Packag. version 3.4-5. https://cran.r-project.org/web/packages/raster/index.html.

69. Wood, S.N. (2011). Fast stable restricted maximum likelihood and marginal likelihood estimation of semiparametric generalized linear models. J. R. Stat. Soc. Ser. B. Stat. Methodol. *73*, 3–36.

70. Muggeo, V.M.R. (2008). segmented: an R package to fit regression models with broken-line relationships. R News *8*, 20–25.

71. Mazerolle, M.J. (2020). AICcmodavg: model selection and multimodel inference based on (Q)AIC(c). R Packag. version 2.3-1. https://cran.r-project.org/web/packages/AICcmodavg/index.html.

72. Gearty, W. (2020). deeptime. R Packag. version 0.5.2. https://doi.org/10.5281/zenodo.3553011.

73. Wickham, H. (2016). ggplot2: Elegant Graphics for Data Analysis (Springer-Verlag).

74. Garnier, S. (2018). viridis: default color maps from "matplotlib." R Packag. version 0.5.1. https://cran.r-project.org/web/packages/viridis/index.html.

75. Robinson, D., Hayes, A., and Couch, S. (2020). broom: convert statistical objects into tidy tibbles. R Packag. version 0.7.3. https://cran.r-project.org/web/packages/broom/index.html.

76. Harrell, F.E., Jr. (2021). Hmisc: Harrell miscellaneous. R Packag. version 4.4-2. https://cran.r-project.org/web/packages/Hmisc/index.html.

77. Venables, W., and Ripley, B. (2002). Modern Applied Statistics with S Fourth (Springer).

78. South, A. (2011). rworldmap: a new R package for mapping global data. R J. *3*, 35–43.

79. Hijmans, R.J. (2019). geosphere: spherical trigonometry. R Packag. version 1.5-10. https://cran.r-project.org/web/packages/geosphere/index.html.

80. Soetaert, K., Petzoldt, T., and Setzer, R.W. (2010). Solving differential equations in R : package deSolve. J. Stat. Softw. *33*, 1–25.

81. Pierce, D. (2019). ncdf4: interface to Unidata netCDF (version 4 or Earlier) format data files. R Packag. version 1.17. https://cran.r-project.org/web/packages/ncdf4/index.html.

82. Michna, P., and Woods, M. (2020). RNetCDF: interface to "NetCDF" datasets. R Packag. version 2.4-2. https://cran.r-project.org/web/packages/RNetCDF/index.html.

Please cite this article in press as: Boag et al., Metabolic tradeoffs control biodiversity gradients through geological time, Current Biology (2021), https://doi.org/10.1016/j.cub.2021.04.021

STAR★METHODS

KEY RESOURCES TABLE

REAGENT or RESOURCE	SOURCE	IDENTIFIER
Deposited data		
Paleobiology Database	https://paleobiodb.org	https://github.com/willgearty/biogradients/blob/v1.0.0/PBDBdata.RData (Paleobiology Database download as described in text - accessed December 2020)
Global Biodiversity Information Facility	https://www.gbif.org	https://www.gbif.org/occurrence/download/0135238-200613084148143 (Global Biodiversity Information Facility download as described in text - accessed December 2020)
HadGEM2-ES	Centre for Environmental Data Analysis (https://data.ceda.ac.uk)	https://data.ceda.ac.uk/badc/cmip5/data/cmip5/output1/MOHC/HadGEM2-ES
Deposited data	This paper	https://github.com/willgearty/biogradients
Software and algorithms		
R computing environment	http://www.r-project.org/; R Development Core Team[64]	v4.0.3
Deposited code	This paper	https://github.com/willgearty/biogradients
rgbif package in R	Chamberlain et al.[65]	v3.4.0
plyr package in R	Wickham[66]	v1.0.2
dplyr package in R	Wickham et al.[67]	v1.0.2
raster package in R	Hijmans et al.[68]	v3.4-5
paleoMap package in R	https://github.com/willgearty/paleoMap	Accessed December 2020
dispeRse package in R	https://github.com/laurasoul/dispeRse	Accessed December 2020
mgcv package in R	Wood[69]	v1.8-33
segmented package in R	Muggeo[70]	v1.3-1
AICcmodavg package in R	Mazerolle[71]	v2.3-1
deeptime package in R	https://github.com/willgearty/deeptime; Gearty[72]	v0.5.2
ggplot2 package in R	Wickham[73]	v3.3.2
viridis package in R	Garnier[74]	v0.5.1
broom package in R	Robinson et al.[75]	v0.7.3
Hmisc package in R	Harrell[76]	v4.4-2
MASS package in R	Venables and Ripley[77]	v7.3-53
rworldmap package in R	South[78]	v1.3-6
geosphere package in R	Hijmans[79]	v1.5-10
deSolve package in R	Soetaert et al.[80]	v1.27.1
ncdf4 package in R	Pierce[81]	v1.17
RNetCDF package in R	Michna and Woods[82]	V2.4-2

RESOURCE AVAILABILITY

Lead contact

Further information and requests for resources should be directed to and will be fulfilled by the Lead Contact, Thomas Boag (thomas.boag@yale.edu)

Materials availability

This study did not generate any reagents or other materials.

Data and code availability

All data and code generated during this study are deposited in the GitHub repository https://github.com/willgearty/biogradients.

Please cite this article in press as: Boag et al., Metabolic tradeoffs control biodiversity gradients through geological time, Current Biology (2021), https://doi.org/10.1016/j.cub.2021.04.021

EXPERIMENTAL MODEL AND SUBJECT DETAILS

This study used fossil occurrence data from the Paleobiology Database (https://paleobiodb.org) and modern biogeographic occurrence data from the Global Biodiversity Information Facility (https://www.gbif.org). No new occurrence data was collected for this study and no physical experiments were conducted.

METHOD DETAILS

Sampling Coverage

To visually assess the sampling coverage of our fossil mollusc occurrence dataset, we plotted the density of occurrences within each time interval (Figure 1). The paleolatitude and paleolongitude coordinates of each occurrence were estimated using the GPlates rotation model.[26] Points were binned within 5-degree by 5-degree hexagons. Some intervals have notable sampling geographic biases, such as a lack of sampling in the Indopacific before the Miocene and limited Southern Hemisphere sampling in several intervals.

To visually assess whether this was a concern at the meta-analysis level, we used the combined modern and fossil mollusc occurrence dataset to calculate the number of occurrences within equal-area latitude bins (12, 24, 45, 90, or 180 bins). We then plotted these occurrence sums (which represent fossil preservation and sampling intensity) against both the bins' mean latitude/paleolatitude (Figure S1A) and mean estimated temperature/paleotemperature (Figure S1B). Despite sampling biases within individual intervals (see above), at the meta-analysis level there is high specimen coverage across all temperatures and paleolatitudes.

Diversity Sensitivity Analyses

Alternative Methodologies

To demonstrate that the observed diversity pattern throughout the geologic record is robust to the methodology used to estimate diversity, we performed additional analyses that cover a wide spectrum of alternative methodologies. We split the occurrence data into a varying number of latitudinal bins (12, 24, 45, 90, and 180 bins), either based on equal areas (each bin has an identical surface area) or equal width (each bin has an equal latitudinal width).We then used these binned occurrences to estimate genus diversity in one of three ways: 1) rangethrough, in which taxa are assumed to occur at all points between their northernmost and southernmost occurrences, then diversity is estimated as in the raw occurrences method; 2) raw occurrences, in which diversity is estimated purely based on the raw number of unique genera that occur in a latitudinal bin; 3) shareholder quorum subsampling (SQS; Locarnini et al.[19]), in which genera are drawn from the occurrences in a given bin until a given "quorum" of the population is achieved based on the frequencies of the genera. We tested quorum values of 0.25, 0.5, and 0.75. For all quorum levels we performed 100 trials. We also tested the inclusion and exclusion of modern data and the use of raw diversity estimates versus proportional diversity estimates (each value is divided by the total generic diversity estimated using the same methodology). Altogether, this resulted in 200 different combined occurrence binning and diversity estimation methodologies. The results of these alternative methodologies were used for several of the following sensitivity analyses.

Sampling Effect on Diversity Estimation

To visually assess whether sampling intensity influenced diversity estimation, we plotted our latitudinal bin diversity estimates from all of the alternative sensitivity methodologies (see above) against the number of specimens/occurrences within the latitudinal bins (Figure S2A). The raw and rangethrough methods suffer from high correlation between diversity estimates and sampling intensity. SQS remedies this to varying degrees at different quorum levels. The 0.25 quorum level allows for high and low diversity estimates across nearly the entire sampling intensity spectrum (30+ specimens). While there are some modern biodiversity hotspots that are notably under-sampled in the fossil record (e.g., the Coral Triangle in the western Pacific Ocean, Figure 1, which was a tectonically active region for most of the time interval studied and has been historically under-sampled by paleontologists), these analyses demonstrate that we have good sampling across sea-surface temperatures. Geographic sampling biases therefore do not appear to have biased our sampling of the relationship we are principally interested in, i.e., that between marine biodiversity and environmental temperature.

HadGEM2-ES Model Results

Past and projected future climate model results are illustrated in Figure 4 to contextualize the relevance of our analyses for future climate change scenarios. We downloaded HadGEM2-ES results from the Centre for Environmental Data Analysis (https://data.ceda.ac.uk/badc/cmip5/data/cmip5/output1/MOHC/HadGEM2-ES). For the equatorial temperature distributions presented in Figure 4, we downloaded monthly sea water potential temperature data spanning the years 1860 (Historical model), 2100 (Representative Concentration Pathway, RCP 4.5 and 8.5[36]) and 2299 (Extended Concentration Pathway, ECP 4.5 and 8.5[37]). For each model scenario in each model year targeted, we computed 5^{th}, 25^{th}, 50^{th}, 75^{th} and 95^{th} percentiles of monthly mean seawater potential temperature for 0-10 m water depth across the central equatorial cells (0.34 to −0.34 degrees latitude).

QUANTIFICATION AND STATISTICAL ANALYSIS

Diversity Sensitivity Analyses

Breakpoint Bootstrap

To assess the robustness of the breakpoint estimation to data outliers, we performed a bootstrap analysis. Each bootstrap consisted of sampling a new set of 198 latitudinal bins from the original compilation with replacement. We made 1000 of these bootstrap

Please cite this article in press as: Boag et al., Metabolic tradeoffs control biodiversity gradients through geological time, Current Biology (2021), https://doi.org/10.1016/j.cub.2021.04.021

datasets and performed a single breakpoint linear regression on each one. We then calculated a weighted mean and standard deviation for the 1000 breakpoint estimates using $1/\sigma^2$ as the weights for the breakpoint estimates. This mean (17.6°C, 290.7K ± 3.4) is not significantly different from the breakpoint of the original analysis (18.3°C, 291.5K ± 3.3).

Model Fitting

To assess the relationship between temperature and proportional generic diversity since the Cretaceous, we fit nine different regression models to the data: linear, linear with one to four breakpoints, quadratic, cubic, quartic, and a generalized additive spline (GAM). We repeated this process 100 times to account for the randomness associated with the bootstrap algorithm used in the breakpoint regression. We then compared the model fits using the corrected Akaike Information Criterion (ΔAICc and AICc weights).[32] To address potential concerns regarding SQS or sampling biases, we repeated this entire model fitting approach using a subset of the alternative methods described above (all analyses used 24 equal-area bins) across three levels of sampling cutoffs (30, 50, and 200 specimens within each bin) (Figure S2B). This approach resulted in essentially no support for a simple linear regression to summarize the relationship between proportional diversity and temperature, regardless of diversity metric or sampling cutoff.

Diversity-Temperature Relationship Sensitivity

Once we had estimated genus diversity for each of alternative methodologies described above, we performed a breakpoint linear regression on the diversity∼temperature data. The estimated breakpoint is robust to binning and diversity estimation methodologies (Figure S3A). We then extracted the slope of the diversity∼temperature relationship for temperatures below the estimated breakpoint, which is also robust to the sensitivity analyses, especially when modern data is included (Figure S3B). Additionally, most slope estimates overlap with the estimate from Roy et al.[1] and the theoretical value from Gillooly and Allen[33] (Figure S3B).

Combined Metabolic Model

We employ a Monte Carlo approach to model diversity-temperature relationships as described in Equations 1, 2, and 3. The distributions used to parameterize the variables in our combined metabolic model are defined in Table S2. $\frac{d\ \ln(S_{Kinet})}{d\ (1000/T)}$ is defined by a linear relationship, as in Allen et al.[14] We sample a uniform distribution of E values 100 times to incorporate uncertainty in the precise slope of this relationship[33] (Table S2). Changes in $\ln\ (S_{Aerob})$ with temperature are defined by the interaction of multiple parameters that are individually described by probability density functions[15] (Table S2). In this study, we focus on how the temperature-sensitivity of hypoxic thresholds (E_o, Equation 3) relates to predicted biodiversity-temperature relationships, defined by a normal distribution as in Penn et al.[15] (Table S2). We solve our model at E_o values corresponding to the mean, mean ± 0.5σ and mean ± 1σ of this normal distribution to produce the analyses presented in Figure 4. A_o and ϕ_{crit} are defined by log-normal distributions as in Penn et al.[15] (Table S2), each sampled 10,000 times. pO_2 is parameterized using a uniform distribution based on modern observations,[19,34] again sampled 10,000 times. The same 10,000 A_o, ϕ_{crit}, and pO_2 values are used in each E_o iteration of our Monte Carlo analyses for consistency. These 10,000 samples are combined to represent a total possible genus pool in our model space, the temperature-sensitivity of which changes with each E_o percentile. $\frac{d\ \ln(S_{Aerob})}{d(1000/T)}$ is computed separately for each E_o percentile using discretization to maximize accuracy, despite the complex non-linear relationships, in the same dimensional space as Allen et al.[14] The distribution of initial values for the differential model is defined based on the best fit model of generic diversity and temperature presented in Figure 3 at the lowest modeled temperature (−1.71°C, 271.44 K), and the 95% confidence intervals of the entire general additive model. Specifically, the mean 95% confidence interval of the segmented linear regression model is used to define the standard deviation of a normal distribution intended to represent approximately the same level of uncertainty illustrated in Figure 3. The intercept of the plotted metabolic model analyses was adjusted to minimize the residual sum of squares between the median metabolic model values (median of distribution at median E_o) and the best fit model presented in Figure 3. 100 initial values were randomly subsampled from this normal distribution and are applied in each E_o iteration of our Monte Carlo analysis. We note that the E_o, A_o, and ϕ_{crit} distributions from Penn et al.[15] are derived from a range of animal phyla, whereas our biodiversity data compilation (Figure 3) is based on molluscs only. We propose (as previous authors have[15]) that the improved sampling density of modern physiological responses that we gain from including non-molluscan taxa improves the accuracy of our model relative to using mollusc data alone. We also show that we can capture the full range of temperature-diversity relationships shown in Figure 3 using the individual mollusc E_o values from the Penn et al.[15] dataset (Figure S4).

Current Biology, Volume *31*

Supplemental Information

Metabolic tradeoffs control biodiversity gradients through geological time

Thomas H. Boag, William Gearty, and Richard G. Stockey

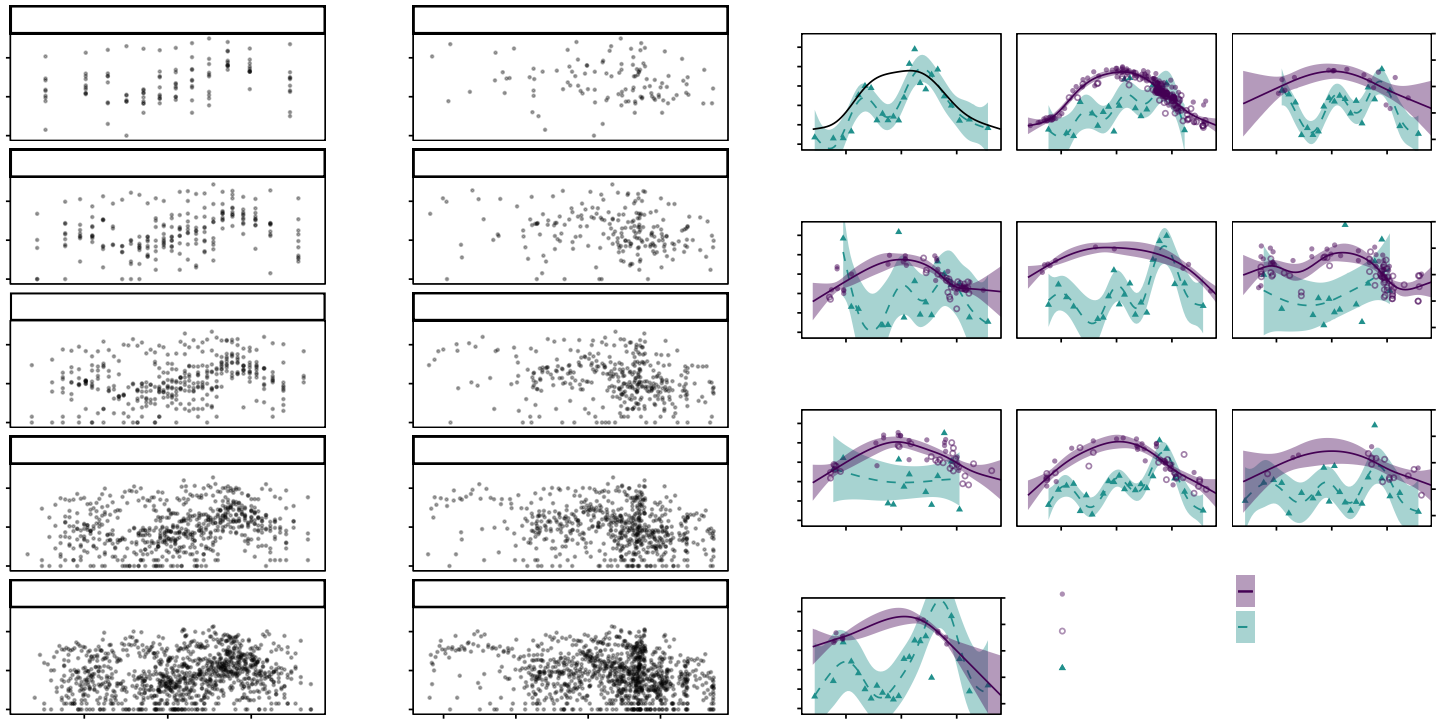

Figure S1. Occurrences and diversity as a function of latitude and temperature, related to Figures 1-2 and STAR Methods. A/B) Plot of number of specimens/occurrences within a latitudinal bin by mean paleolatitude (A) or mean SST (B) of the bin. Points include all latitudinal bins from the combined modern and fossil mollusc occurrence dataset. Vertical panels indicate number of equal-area latitudinal bins. At the meta-analysis level, there is high specimen coverage across all temperatures and paleolatitudes.

C) Modern sea surface temperature and estimated paleotemperature plotted by latitude (purple circles) with best fit splines (solid purple lines). Filled circles represent temperature estimates based on marine proxies, while open circles represent temperature estimates based on terrestrial proxies. Estimated SQS genus diversity (in proportion of total SQS genera) is also plotted by latitude (green triangles) with best fit splines (dashed green lines). Envelopes indicate 95% confidence intervals. Note that these temperature regression splines are used in all analyses to interpolate temperature to latitudes without proxies, but no interpolation is performed on diversity data and only latitudes with diversity data are used in analyses. Diversity regression splines are for display purposes only.

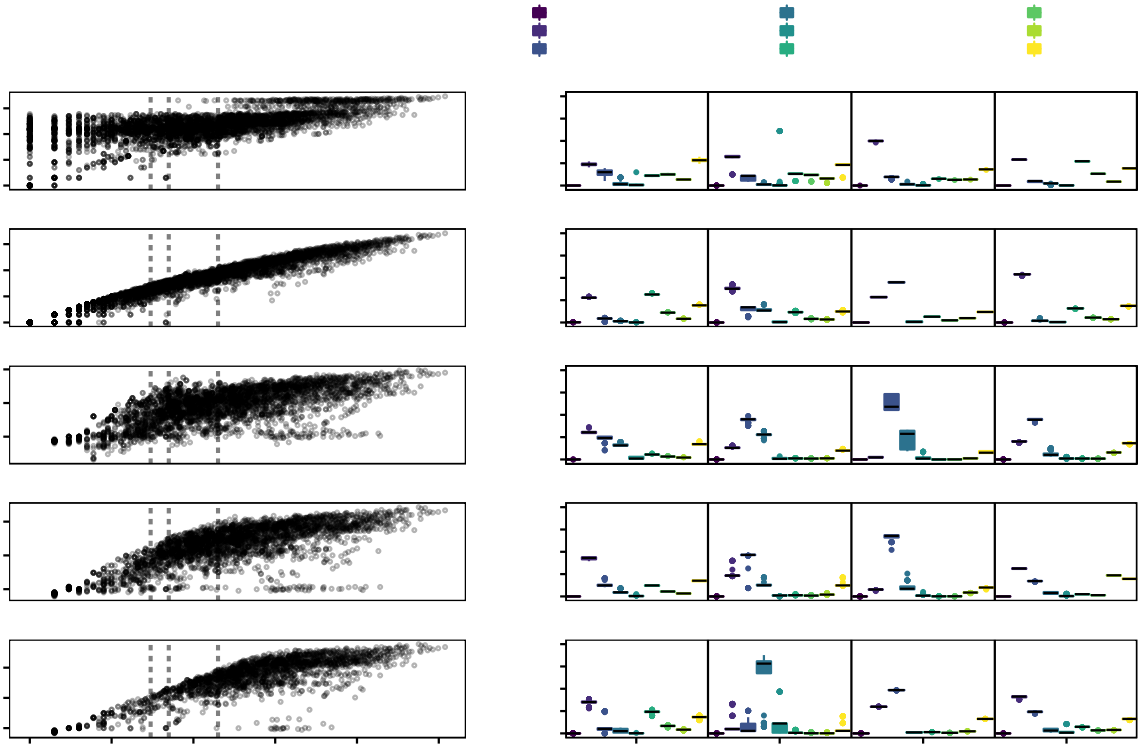

Figure S2. Effects of within-bin sampling on results, related to Figure 3 and STAR Methods.

A) Plot of estimated diversity by number of specimens/occurrences within a latitudinal bin. Includes results across all sensitivity permutations (see Diversity Sensitivity Analyses in Supplemental Methods). Vertical dashed lines represent sensitivity cutoffs of 30, 50, and 200. Raw and rangethrough methods suffer from high correlation between diversity estimates and sampling intensity. SQS remedies this to varying degrees at different quorum levels. The 0.25 quorum level allows for high and low diversity estimates across nearly the entire sampling intensity spectrum (30+ specimens).

B) Model fit comparisons for different diversity estimation methods and sampling cutoffs. All analyses used 24 equal-area latitudinal bins as in the main analysis. Each set of models was run 100 times to account for the bootstrap nature of the breakpoint analyses. A simple linear model has essentially no support regardless of data treatment.

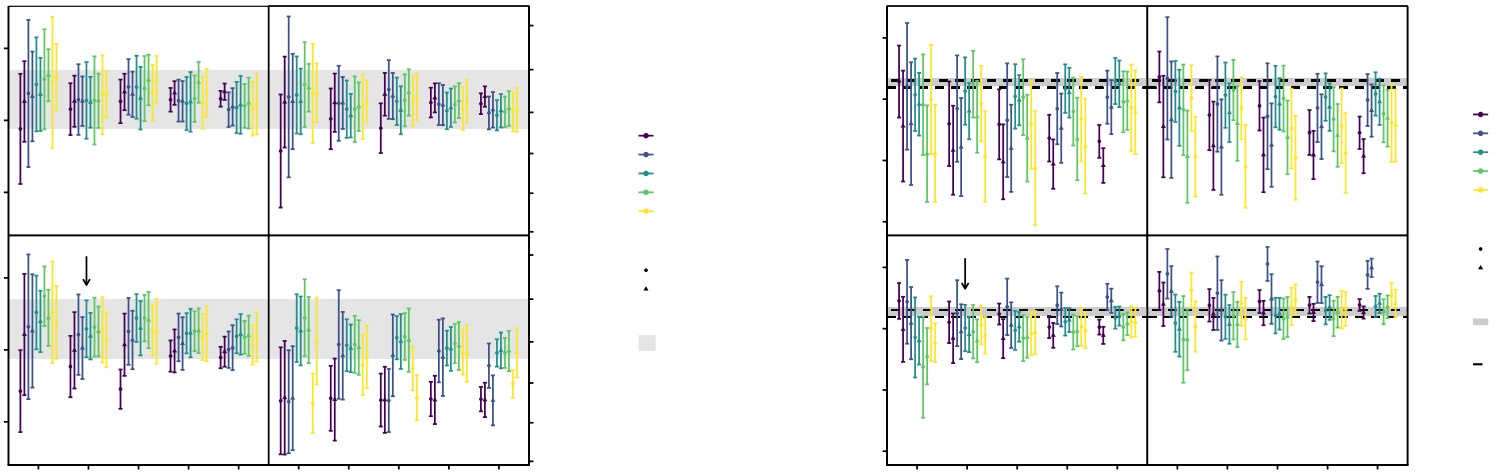

Figure S3. Most methods for diversity estimation result in similar best breakpoints and slopes for the diversity~temperature relationship, related to Figure 3 and STAR Methods.

A) Sensitivity analysis of diversity~temperature breakpoint. Diversity is calculated as the ln(Percent Total Diversity), and temperature is calculated as 1000/T. The colors of the points represent different diversity metrics, the symbols of the points represent different latitudinal band types, and the error bars associated with the points represent ±1.96σ. The point corresponding to the methods of this study are indicated in the bottom-left panel and the range of the error associated with that point is indicated by the grey band in all four panels.

B) Sensitivity analysis of diversity~temperature slope. Results show most methods for diversity estimation result in the same diversity~temperature slope at temperatures below the fitted breakpoint, which corresponds with both the Roy et al.[S1] empirical estimate (grey region) and the Gillooly and Allen[S2] theoretical range (dashed lines). For the slope estimation, diversity is calculated as the ln(Diversity), and temperature is calculated as 1000/T. Points and errors bars as in A. The point corresponding to the methods of this study are indicated in the bottom-left panel.

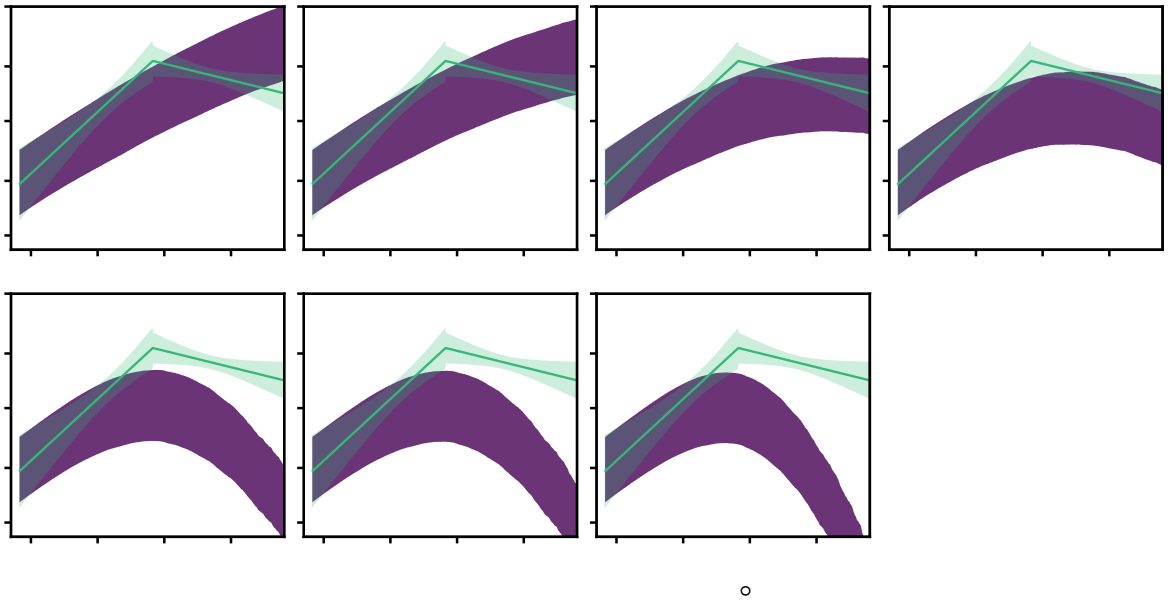

Figure S4: **Sensitivity analysis of combined metabolic model using only mollusc E_o values, related to Figure 4 and STAR Methods.** All other model parameters are the same as those illustrated in Figure 4.

Model	ΔAICc	AICc weight
Linear	23.2	0
One Breakpoint	**0**	**0.3**
Two Breakpoints	**0.51**	**0.24**
Three Breakpoints	**1.35**	**0.16**
Four Breakpoints	6.83	0.01
Quadratic	3.41	0.06
Cubic	4.47	0.03
Quartic	5.32	0.02
GAM	**1.15**	**0.17**

Table S1. Median ΔAICc and AICc weights for each of the nine models compared for the main analysis, related to Figure 3 and STAR Methods. Bold indicates models with < 2 ΔAICc (substantial support). There is essentially no support for a simple linear model. See Figure S2B for complete model comparison results.

Variable	Distribution Type	Parameterization	Unit	Reference
E	uniform	min = 0.6 max = 0.7	eV	S2
A_o	log-normal	μ = 3.01 σ = 0.49	atm^{-1}	S3
E_o	normal	μ = 0.41 σ = 0.29	eV	S3
ϕ_{crit}	log-normal	μ = 1.10 σ = 0.42		S3
pO_2	uniform	min = 0.1957 max = 0.2146	atm	S4, S5

Table S2. Variable distributions used in combined metabolic model, related to STAR Methods.

Supplemental References

S1. Roy, K., Jablonski, D., Valentine, J.W., and Rosenberg, G. (1998). Marine latitudinal diversity gradients: Tests of causal hypotheses. Proc. Natl. Acad. Sci. U. S. A. 95, 3699–3702.

S2. Gillooly, J.F., and Allen, A.P. (2007). Linking global patterns in biodiversity to evolutionary dynamics using metabolic theory. Ecology 88, 1890–1894.

S3. Penn, J.L., Deutsch, C., Payne, J.L., and Sperling, E.A. (2018). Temperature-dependent hypoxia explains biogeography and severity of end-Permian marine mass extinction. Science 362.

S4. Locarnini, R.A., Mishonov, A. V., Antonov, J.I., Boyer, T.P., Garcia, H.E., Baranova, O.K., Zweng, M.M., Paver, C.R., Reagan, J.R., Johnson, D.R., et al. (2013). World ocean atlas 2013. Volume 1, Temperature.

S5. Boag, T.H., Stockey, R.G., Elder, L.E., Hull, P.M., and Sperling, E.A. (2018). Oxygen, temperature and the deep-marine stenothermal cradle of Ediacaran evolution. Proc. R. Soc. B Biol. Sci. 285.